AN ANALYSIS OF THE BILGE KEEL ROLL DAMPING COMPONENT MODEL

Christopher C. Bassler, Arthur M. Reed
Naval Surface Warfare Center, Carderock Division, USA

ABSTRACT

Since the 1970s, component-based frequency-domain models based on Ikeda's method have been used to predict roll damping. These are based on data from conventional wall-sided hull forms at small roll angles. The limits of applicability for large roll amplitudes and unconventional hull form geometries are not well understood. Bilge keel roll damping component predictions are computed using Ikeda's formulas for three vessels. Comparisons were made to highlight differences in bilge keel roll damping components for modern hull forms and to identify limits of application with roll amplitude. The bilge keel-hull interaction damping component is influenced by both bilge keel size and hull proportions, resulting in unreasonable behavior at larger roll amplitudes and roll frequencies. A simple model for the bilge keel wave-making component is proposed and examined to determine when this component should be considered.

Keywords: *roll damping, bilge keel size, large-amplitude roll, bilge keel wave-making*

1. INTRODUCTION

Roll damping is essential to accurately describe the motions of a ship, particularly when operating in moderate to extreme sea conditions, and is most significant for parametric or synchronous roll phenomena (Bassler, 2008a). Roll damping is a complex process of energy transfer which affects the amplitude of motion. Damping for roll motion is dominated by viscous effects and the interaction of the ship with the free surface, wind, and waves presents a difficult problem to accurately model. Bilge keels have been used for many years on ships to increase damping and reduce the severity of roll motions experience by a ship in waves. Because ship motions are more severe and large roll angles may occur in moderate to extreme sea conditions — with the possibility of crew injury, cargo damage, or even capsize, it is important to understand how damping functions for these conditions.

Roll damping models have been proposed using both time-domain and frequency-domain formulations. The first roll damping models were developed in the frequency domain. In the 1950-60s, the first scientific investigations to study the individual physical aspects of ship roll damping were performed (Sasajima, 1954; Tanaka, 1957, 1958, 1959, 1961; Martin, 1958; Kato, 1958, 1965). In the 1970s, a component method was developed to more accurately describe the roll damping of ships and integrate methods to describe distinct physical phenomena to determine total roll damping (Ikeda, et al, 1978a, 1978b, 1978c, 1978d, 1978e; Himeno, 1981). The method decomposed ship roll damping into seven parts and combined them linearly to calculate roll damping for conventional hull forms at small angles, with and without forward speed. The component approach compared well to experimental data and was the first comprehensive model for ship roll damping with consideration of distinct physical phenomena. Schmitke (1978) also developed a

NOMENCLATURE

A_ϕ	mass moment of inertia in roll	Cϕ	roll restoring component
b_{BK}	bilge keel span (m)	CD	drag coefficient
B	beam (m)	d	draft (m)
B_{44}	linearized total roll damping	dBK	distance from the free surface to the bilge keel (m, positive below waterline)
B_1	linear roll damping component	Fn	Froude number
B_2	quadratic roll damping component	g	gravitational acceleration (m/s2)
B_3	cubic roll damping component	H0	half breadth/draft = B/(2d)
B_F	roll friction damping component	KC	Keulegan-Carpenter number = πrϕ/bBK
B_E	roll eddy damping component	L	ship length (m)
B_L	roll lift damping component	OG	distance from calm water level to roll axis (m, positive down)
B_W	roll wave-making damping component	r	distance from roll axis to bilge keel (m)
B_{BK}	bilge keel roll damping component	R	radius of the bilge circle (m)
B_{BKN}	bilge keel normal damping component	T	roll period (s)
B_{BKH}	bilge keel-hull interaction damping	U	forward speed (m/s)
B_{BKW}	bilge keel wave-making damping	ν	kinematic viscosity (m2/s)
B_ϕ	cubic roll damping component	ρ	fluid density (kg/m3)
C_B	block coefficient	σ	sectional area coefficient
C_M	midship section coefficient	ϕ	roll amplitude (radians)
C_P	pressure coefficient	ω	roll frequency (rad/s)

component based formulation, dividing roll damping into contributions from the bilge keel, eddy-making, hull friction, and appendages (in addition to bilge keels) at zero speed. The component-based model, or some derivative, has been state-of-the-art for roll damping computations since its development.

In time-domain formulations, the damping term may be comprised of both linear and nonlinear components (Haddara, 1973; Lewison, 1976; Dalzell, 1978; Himeno, 1981; Cotton & Spyrou, 2000; Spyrou & Thompson, 2000). However, roll decay data regression analysis is typically used to determine the components, without considerations to distinct physical phenomena. Frequency-domain models were developed with considerations for physical phenomena, but it is difficult to equate these components to properly determine non-linear damping terms in the time-domain.

Since the 1970s, methods based on the component analysis model have been used to predict roll damping. These semi-empirical frequency-domain models are based on data from conventional wall-sided type hull forms at small roll angles. Because ship response was considered only in small to moderate wave conditions, the original calculations were only performed for roll amplitudes up to 10 degrees, and later extended to 15 degrees. Although these limitations were acknowledged in the development, the limits of applicability are not well known for ships at larger roll amplitudes and with more modern hull form geometries.

Additional work has been performed to extend the application of the component model. De Kat (1988) computed the roll damping coefficients at the natural roll frequency and then used these for other roll frequencies. Blok & Aalbers (1991) decomposed the roll damping due to the bilge keels into two components, the lift on the bilge keel and the eddy generation from the bilge keels. Other methods have been developed where each component is determined for zero speed and then forward speed corrections are applied. Ikeda (2004) also detailed improvements to his method to determine optimal location for placement of the bilge keels. Changes have also been made to extend Ikeda's method to high-speed planning craft, with modifications to the lift component (Ikeda & Katayama, 2000), and high-speed multi-hull vessels, with modifications to the wave-making, eddy, and lift components (Katayama, et al., 2008). For these high-speed vessels, predictions were performed for speeds up to $Fn = 0.6$.

Some derivative of the method developed by Ikeda, et al. (1978d) is used in most modern potential flow codes to predict ship motion performance. Predictions using common potential flow codes have shown significant variation in trends for roll decay results including forward speed compared to experimental results, especially for more modern hull form geometries, such as the ONR Topside Series (Bassler, 2007). For these more modern ship types, discrepancies between the predicted roll moment and experimental results are due in part to the difficulty of calculating the eddy and bilge keel components in a potential flow simulation (Bassler, 2008b). This presents inherent limitations for the application of modern ship motions simulation tools (Beck & Reed, 2001).

Improvements have also been made in roll damping predictions using viscous flow codes (Yeung, et al., 1998, 2000; Roddier, et al., 2000; Seah, 2007; Seah & Yeung, 2008) and unsteady RANS codes (Korpus & Falzarano, 1997; Miller, et al., 2002, 2008; Wilson, et al., 2006), but these simulation tools require long computational times. Because of the widespread use of faster, potential flow-based codes, particularly early in the ship design process, the limitations for roll damping predictions must be better understood.

To determine roll damping for different ship types, experimental results remain necessary. Experiments have been performed for naval vessels at the United States

Experimental Model Basin (EMB 1920, 1931), a predecessor of the David Taylor Model Basin, for cylindrical sections (Stefun, 1955; Vugts, 1968; Gersten, 1969); for a cargo ship, Series 60 hull forms with varied C_B and a tanker (Ikeda, et al. 1978a, 1978b, 1978c, 1978d, 1978e; Himeno, 1981); for modern naval hull forms (Bishop, et al., 2005; Hayden, et al., 2006; Bassler, et al., 2007); and for ships with instrumented appendages (Atsavapranee, et al., 2007; Grant, et al. 2007; Etebari, et al., 2008).

2. COMPONENT MODEL FOR ROLL DAMPING

A simple model for ship roll motion employs the single degree of freedom equation,

$$A_\phi \ddot{\phi} + B_\phi\left(\dot{\phi}\right) + C_\phi \phi = M_\phi\left(\omega t\right) \tag{1}$$

where the damping term may be decomposed into both linear and nonlinear components.

$$B_\phi\left(\dot{\phi}\right) = B_1\dot{\phi} + B_2\dot{\phi}\left|\dot{\phi}\right| + B_3\dot{\phi}^3 + \ldots \tag{2}$$

Because of the difficulty in analyzing nonlinear roll damping, it was assumed the nonlinear terms could be approximated using a linearized coefficient

$$B_\phi\left(\dot{\phi}\right) = B_{44}\dot{\phi} \tag{3}$$

and the equivalent linear damping coefficient, B_{44}, could be obtained using a linear combination of physical components, each as a function of roll amplitude, roll frequency, and forward speed (Ikeda, et al., 1978e, Himeno, 1981).

$$B_{44} = B_F + B_E + B_L + B_W + B_{BK} \tag{4}$$

The components include both empirical (friction, B_F; eddy, B_E; and wave-making B_W,) and semi-empirical (hull lift, B_L; bilge keel normal force, B_{BKN}; and bilge keel-hull interaction B_{BKH}) formulations. The bilge keel wave-making component, B_{BKW}, was neglected.

Even at small roll amplitudes, the bilge keel damping components contribute a large portion to the total damping and these contributions increase with both roll amplitude (Figure 1) and roll frequency. The bilge keel-hull interaction component is assumed not to depend on forward speed (Ikeda, et al., 1978b).

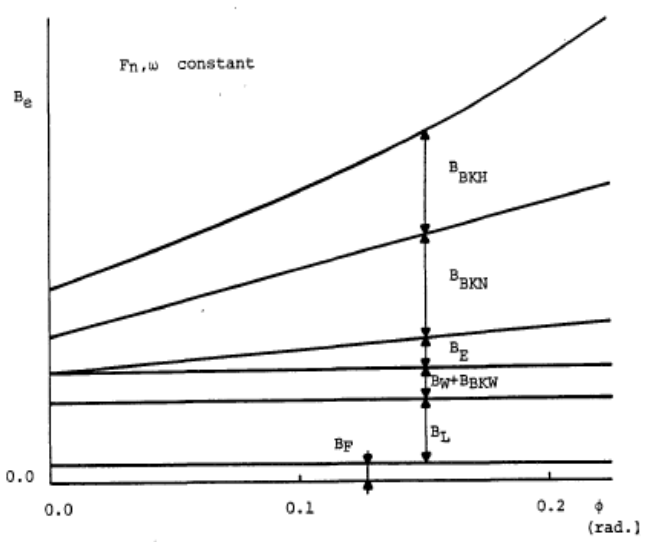

Figure 1. Relative magnitude of roll damping components dependent on roll amplitude (Himeno, 1981).

2.1 Bilge Keel Damping

A formulation for the bilge keel damping component was presented in Ikeda, et al. (1978a, 1978b, 1978e). The bilge keel damping component is comprised three sub-components: the normal force on the bilge keel, B_{BKN}, the bilge keel-hull interaction, B_{BKH}, and wave-making due to the bilge keels, B_{BKW}.

$$B_{BK} = B_{BKN} + B_{BKH} + B_{BKW} \tag{5}$$

Both the bilge keel normal force and bilge keel-hull interaction components are functionally dependent on the Keulegan-Carpenter number, KC, (Keulegan & Carpenter, 1958). Based on the formulation for r and R given by Ikeda, et al. (1978e), the bilge keel is assumed to be attached to the hull at the midpoint of the quarter circle circumscribed by the bilge circle radius (Figure 2). These

parameters are used in both the bilge keel normal force and bilge keel-hull interaction components. Additional details regarding the equations used to calculate the bilge keel normal force and bilge keel-hull interaction components are presented in the Appendix.

Bilge Keel Normal Force. This component is related to the drag which occurs on the bilge keels as they oscillate in a fluid. The formula for the bilge keel normal force component of roll damping is given by Ikeda, et al. (1978a). The bilge keel normal force component at zero speed, B_{BKN0}, is given by

$$B_{BKN0} = \frac{8}{3\pi}\rho r^2 {b_{BK}}^2 \omega f^2 \left[\frac{22.5}{\pi f} + 2.4\frac{r\phi}{b_{BK}}\right] \quad (6)$$

where ρ is the fluid density, r is the distance from the roll axis to the bilge keel, b_{bk} is the bilge keel span, ω is the roll frequency, ϕ is the roll angle, and f is an empirical function of the section coefficient (see Appendix). The total bilge keel normal force component, B_{BKN}, is given by

$$B_{BKN} = B_{BKN0} + \frac{\pi}{2}\rho {b_{BK}}^2 r^2 U \quad (7)$$

where U is the forward speed and the other terms are defined above.

Bilge Keel-Hull Interaction. This component is related to the pressure change on the hull surface due to the presence of the bilge keels. The formula for the bilge keel-hull interaction component of roll damping is given by Ikeda, et al. (1978b). The bilge keel-hull interaction component, B_{BKH}, is given by

$$B_{BKH} = \frac{4}{3\pi} r^2 d^4 f^2 \omega\phi \int C_p \cdot l dG \quad (8)$$

where d is the draft, C_p is the pressure coefficient on the local section of the hull due to the presence of the bilge keel, l is the moment lever for a ship section, and these are integrated over the girth of the hull, and the other terms are defined above.

Bilge Keel Wave-Making. This component is related to the effects of the bilge keel from the free surface. The wave-making component of bilge keel damping, B_{BKW}, is difficult to calculate. This is partially due to the phase difference between the wave-making from the ship and the wave-making from the bilge keel, which may result in either additive or subtractive effects to the hull damping (Ikeda, et al., 1978d; Himeno, 1981). For bilge keels with b_{BK} = $B/60$ to $B/80$, Himeno (1981) assumes that the bilge keel wave-making component may be neglected because at small roll amplitudes, the interaction with the free surface will be negligible, resulting in a small magnitude relative to the other damping components. However, Himeno cautions that for ships with larger bilge keels, such as warships, the bilge keel wave-making component may be significant. This component is also expected to be more important for larger roll amplitudes, where the bilge keel interaction with the free surface is greater.

For vessels which feature larger bilge keels, such as the ONR Topside Series hull form, the wave-making damping component may be non-trivial and added mass effects of the bilge keel should also be considered. Additional considerations also must be made for large amplitude roll motion. The Ikeda component model is based on small roll amplitudes. For larger roll amplitudes, where the bilge keel approaches closer to the free surface, and lower roll frequencies, the bilge keel wave-making component may be significant.

A formulation of the bilge keel wave-making damping component is not presented in this paper. However, to help determine when this component should be considered, a simple model is examined to provide an estimate of the relative order of magnitude of this component for different roll amplitudes and frequencies.

The following model is proposed to examine the bilge keel wave-making component at zero speed, B_{BKW0}. In this formulation, the bilge keel may be considered as a source, pulsing at a frequency, ω, at a

depth relative to the free surface, d_{BK}, based on the roll amplitude, ϕ.

$$B_{BKW\,0} \sim C_{BK}\left(b_{BK}\right)\cdot\exp\left(-\frac{\omega^2}{g}d_{BK}\left(\phi\right)\right) \quad (9)$$

where the source strength, C_{BK}, will be a function of the size of the bilge keel span, b_{BK}. For simplicity, C_{BK} is assumed to be the ratio of the bilge keel span to ship beam. The damping was assumed to be zero for zero roll amplitude. The distance from the free surface to the bilge keel, d_{BK}, is given by

$$d_{BK}(\phi)=r\cdot\left[\left(\frac{(2d/B)}{\sqrt{1+(2d/B)^2}}\right)\cos\phi-\sin\phi\cdot\left(\frac{1}{\sqrt{1+(2d/B)^2}}\right)\right] \quad (10)$$

where d is the draft, B the beam, and ϕ the roll angle.

The derivation of the expression for bilge keel depth (Figure 2) is discussed in the Appendix. This formulation is valid for conventional ships where the draft is larger than the bilge radius — a limitation that could be overcome by providing the actual location of the bilge keel rather than using Ikeda, et al.'s empirical relationships for the location of the bilge keel. For this simple model, forward speed effects are not considered.

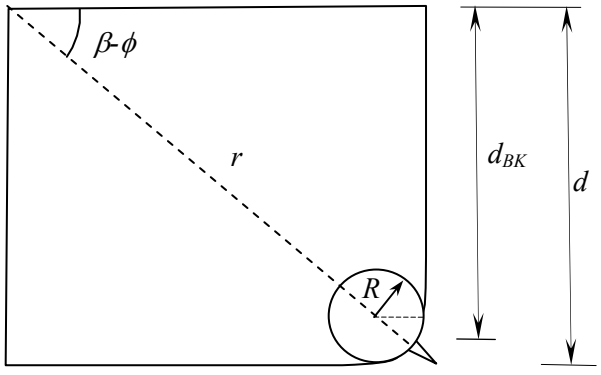

Figure 2. Illustration of the bilge keel depth, d_{BK}, as a function of roll angle, ϕ, and distance from the roll axis to the bilge keel, r, for the half-midship section of a conventional hull form.

3. HULL FORMS

Three hull forms were chosen for this investigation. Two of the hull forms, a cargo ship and Series 60, were tested and analyzed during the original development of the roll damping component model (Ikeda, et al., 1978d; Himeno, 1981). Both hull forms represent conventional ship types (IMO, 2008). These two hull forms provide baselines for examining trends, both at larger roll amplitudes than the original studies and for different ship geometry. The ONR topside series was used to provide analysis of a more modern naval hull form, representing an unconventional ship type.

To calculate the roll damping components and enable direct comparison, without consideration for the difficulties of scaling viscous effects (Gersten, 1971), the vessel particulars were normalized to a nominal model of 3 m length.

3.1 Cargo Ship

The cargo ship hull form was given in Ikeda, et al. (1978d) and Himeno (1981). Of the three ships investigated, the cargo ship with bulbous bow (Table 1) represents the most conventional ship, with the highest block coefficient, C_B, and midship section coefficient, C_M.

Table 1. Cargo ship model particulars

L (m)	3.0
B (m)	0.4783
d (m)	0.1957
Δ (kg)	199.84
C_B	0.7119
C_M	0.9905
b_{BK}/B	0.0159

3.2 Series 60

The Series 60 hull form (Figure 3) was designed at the David Taylor Model Basin and

intended to provide a systematic variation of single-screw merchant ship hull forms (Todd, 1953). The Series 60 C_B = 0.60 variant was chosen, as it represents a middle hull form of the three ship investigated. The model dimensions given in Ikeda, et al. (1978b, 1978d) were again normalized to 3 m length (Table 2).

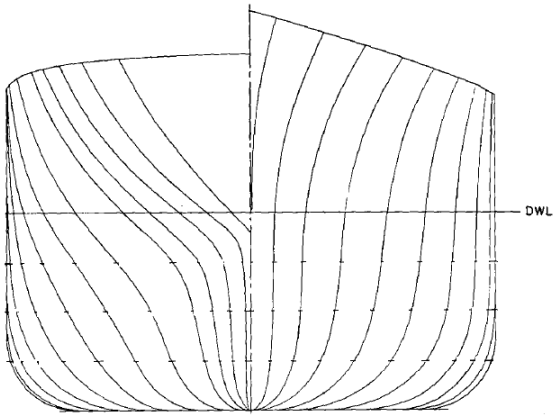

Figure 3. Series 60 hull form body plan.

Table 2. Series 60 ship model particulars.

L (m)	3.0
B (m)	0.3958
d (m)	0.1603
Δ (kg)	111.779
C_B	0.60
C_M	0.977
b_{BK}/B	0.0228

3.3 ONR Topside Series

The Office of Naval Research ONR Topside Series (Figure 4) was designed at the David Taylor Model Basin (Bishop, et al., 2005). The hull forms represent a modern naval combatant ship design and feature a common below waterline geometry, with varied topside shapes, including wall-sided, flared, and tumblehome topsides. The given ship particulars are normalized using the geometry of DTMB Model 5613 from Bishop, et al. (2005) and Bassler, et al. (2007). Because the components examined for this investigation only consider hull form shape below the waterline, only the common underbody dimensions are provided (Table 3). The hull form series is characterized by a lower block coefficient, C_B, shallower draft, and larger bilge keels relative to the cargo ship and Series 60 hull forms.

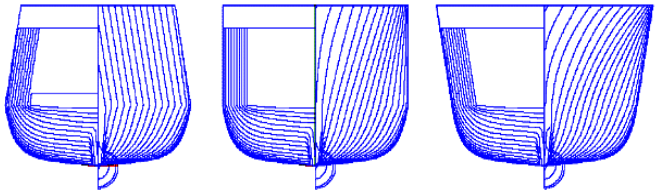

Figure 4. ONR Topside Series hull form body plans, tumblehome (left), wall-sided (middle) and flared (right).

Table 3. ONR Topside Series ship model particulars.

L (m)	3.0
B (m)	0.366
d (m)	0.1073
Δ (kg)	63.119
C_B	0.535
C_M	0.837
b_{BK}/B	0.0663

3.4 Conditions

Roll amplitudes from ϕ = 0 to 30 degrees and roll frequencies from ω = 1 to 7 rad/s were investigated. The effects of forward speed were not examined—bilge keel-hull interaction component was not considered to be dependent on forward speed. Kinematic viscosity, ν, was assumed to be 10^{-6} m^2/s, for fresh water at 20°C. For simplification, the roll axis, OG, was assumed to be at the vertical center of gravity, and therefore, could be neglected. All of the component evaluations were performed for the respective normalized model dimensions given above.

4. RESULTS

All plots are presented as non-dimensional damping components, where

$$B_{BK} = B_{BK} \frac{\sqrt{\frac{B}{2g}}}{\rho \nabla B^2} \qquad (11)$$

In the case of the bilge keel wave-making component, the damping is inherently non-dimensional. Unless otherwise indicated, results are for the given physical model dimensions. The roll frequencies are given at model scale.

4.1 Bilge Keel Normal Force Component

Using the formulation by Ikeda, et al. (1978a), the bilge keel normal force component of roll damping was determined for the three ships for a range of roll amplitudes and frequencies. Figure 5, 6, and 7 give the non-dimensional bilge keel normal force component for the cargo ship, Series 60 C_B = 0.60, and ONR Topside Series, respectively.

All three figures are plotted to the same scale on the ordinate to illustrate how the damping varies between the three hull forms. The bilge keel normal force damping for the cargo ship and the Series 60 models are quite comparable, while the damping is significantly larger for the ONR Topside Series, primarily due to its larger bilge keel span relative to the other two hulls — roughly three times larger. In all cases, the bilge keel normal force is linear in both amplitude and frequency.

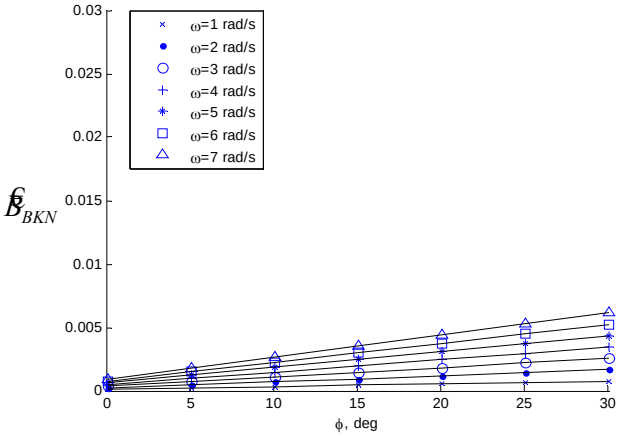

Figure 5. Cargo ship, bilge keel normal force damping component vs roll amplitude, $Fn = 0$.

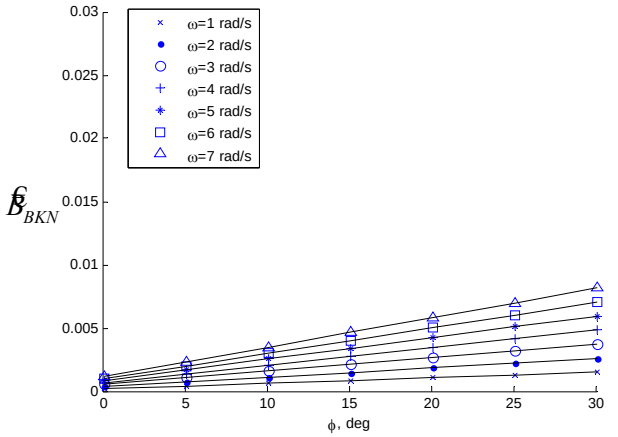

Figure 6. Series 60, bilge keel normal force damping component vs roll amplitude, $Fn = 0$.

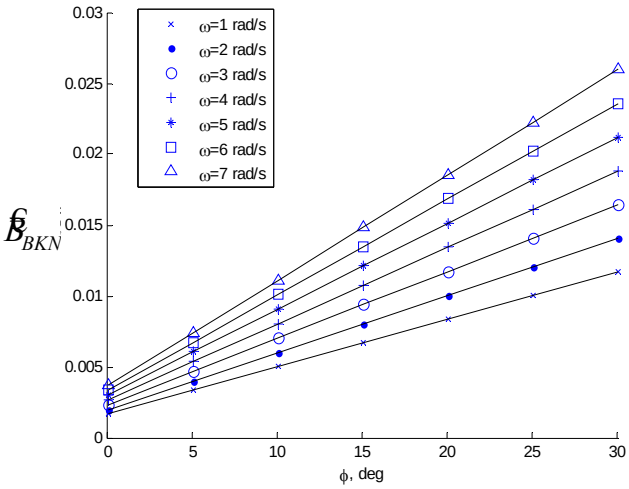

Figure 7. ONR Topside Series, bilge keel normal force damping component vs roll amplitude, $Fn = 0$.

4.2 Bilge Keel-Hull Interaction Component

Using the formulation of Ikeda, et al. (1978b), the bilge keel-hull interaction component of roll damping was determined for the three ships for a range of roll amplitudes and frequencies. Figures 8, 9, and 10 give the non-dimensional bilge keel-hull interaction damping for the cargo ship, Series 60 C_B = 0.60, and ONR Topside Series, respectively.

Figures 8 and 9 are plotted to the same scale on the ordinate to illustrate how the roll damping varies between the two conventional hull forms, while the scale on Figure 10 is an order of magnitude larger.

For the cargo ship and Series 60 hulls, the bilge keel-hull interaction damping is an order of magnitude smaller than the bilge keel normal force damping, while for the ONR Topside Series, the bilge keel-hull interaction damping is two orders of magnitude smaller than the bilge keel normal force damping.

The bilge keel-hull interaction damping is linear in roll frequency, but for the cargo ship and Series 60 hulls the integral of the pressure coefficient over the girth of the hull surface increases with a power of roll amplitude. However, for the ONR Topside Series, the bilge keel-hull interaction damping initial increases with a power of roll amplitude, but then levels off to essentially constant for larger roll amplitudes.

4.3 Component Behavior with Bilge Keel Size

The bilge keel-hull interaction component of roll damping is presented as a function of the bilge keel span to beam ratio for two ships, the Series 60 hull (Figures 11 and 12) and the ONR Topside Series (Figures 13 and 14), for a range of roll amplitudes and frequencies. Both the cargo ship and Series 60 hull forms exhibited similar trends for the bilge keel-hull interaction damping as a function of bilge keel span. In all cases, only the bilge keel span was varied. For the original hull forms examined in the development of the component roll damping model, the ratio of bilge keel span to beam was less than 3 percent. For modern hull forms, the bilge keel span to beam ratio can range up to 10 percent.

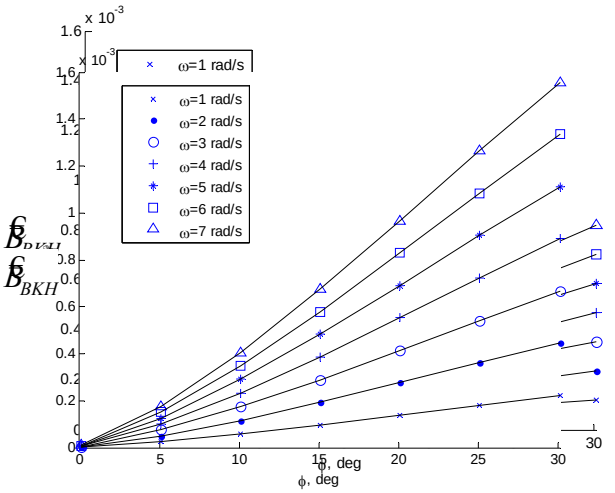

Figure 8. Cargo ship, bilge keel-hull interaction damping component vs roll amplitude, $Fn = 0$.

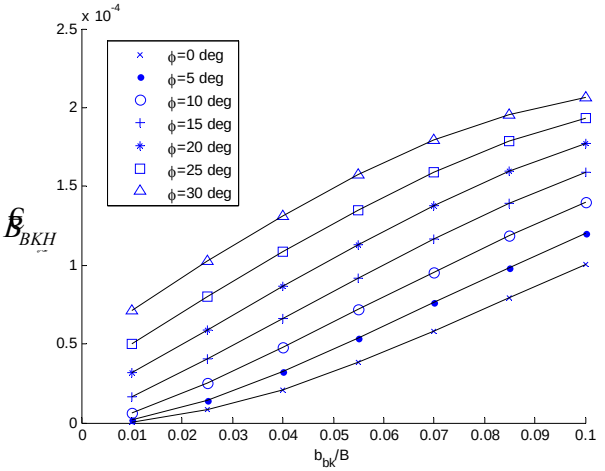

Figure 9. Series 60, bilge keel-hull interaction damping component vs roll amplitude, $Fn = 0$.

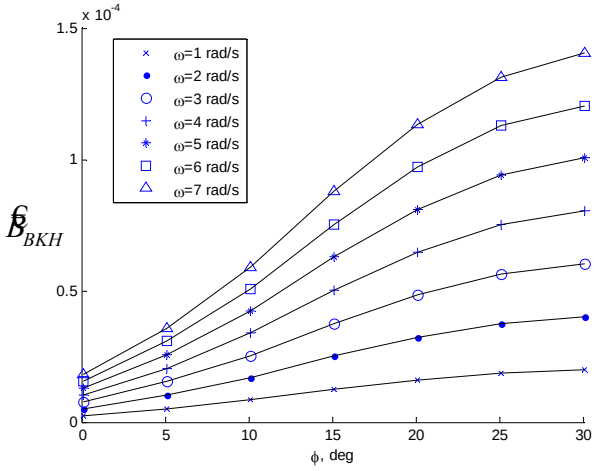

Figure 10. ONR Topside Series, bilge keel-hull interaction damping component vs roll amplitude, Fn = 0 (note: different scale for damping magnitude).

Figures 11 and 13 present the bilge keel-hull interaction damping at the lowest roll frequency; they are plotted to the same scale on the ordinate to illustrate how the roll damping varies with bilge keel size for the Series 60 and the ONR Topside Series hull forms, respectively. Figures 12 and 14 present the bilge keel-hull interaction damping at the highest roll frequency. They show that the bilge keel-hull interaction damping is an order of magnitude smaller for the ONR Topside Series compares to the Series 60 hull form. For both hull forms, increasing roll frequency resulted in an increase in the bilge keel-hull interaction damping by an order of magnitude.

At smaller roll amplitudes, the bilge keel-hull interaction damping increases linearly or as a power of the bilge keel span, depending on the magnitude of the roll. However, for larger bilge keels at larger roll amplitudes the damping begins to plateau (Figures 11 and 12) and then decrease (Figures 13 and 14).

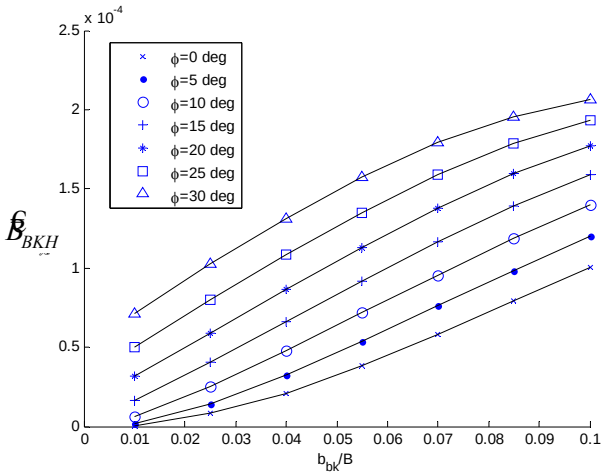

Figure 11. Series 60, bilge keel-hull interaction damping component vs ratio of bilge keel span to beam, ω = 1 rad/s, Fn = 0.

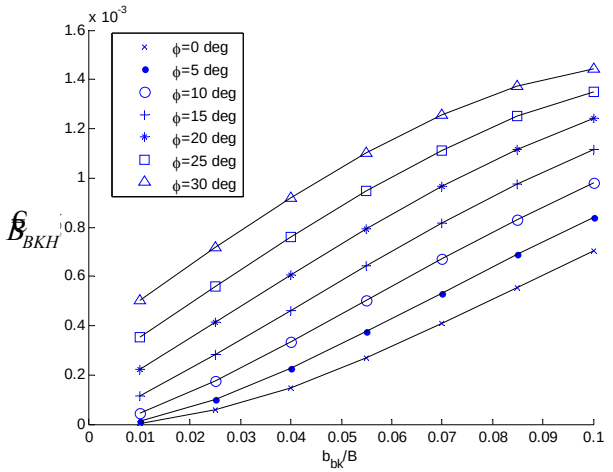

Figure 12. Series 60, bilge keel-hull interaction damping component vs ratio of bilge keel span to beam, ω = 7 rad/s, Fn = 0 (note: different scale for damping magnitude).

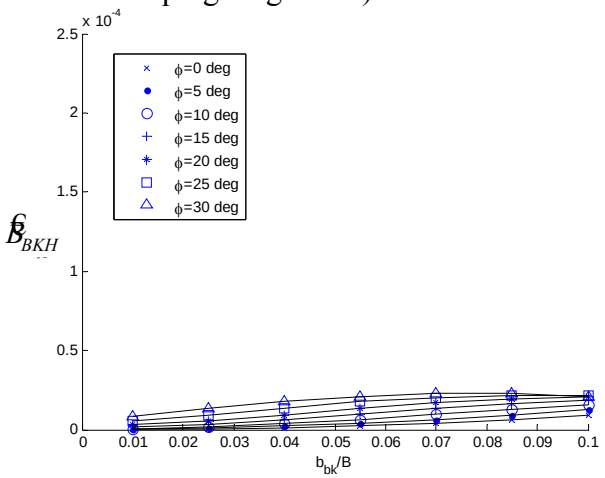

Figure 13. ONR Topside Series, bilge keel-hull interaction damping component vs ratio of bilge keel span to beam, ω = 1 rad/s, Fn = 0.

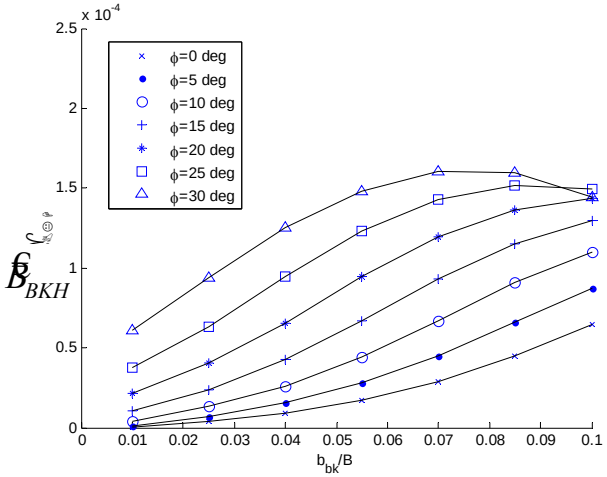

Figure 14. ONR Topside Series, bilge keel-hull interaction damping component vs ratio of bilge keel span to beam, $\omega = 7$ rad/s, $Fn = 0$.

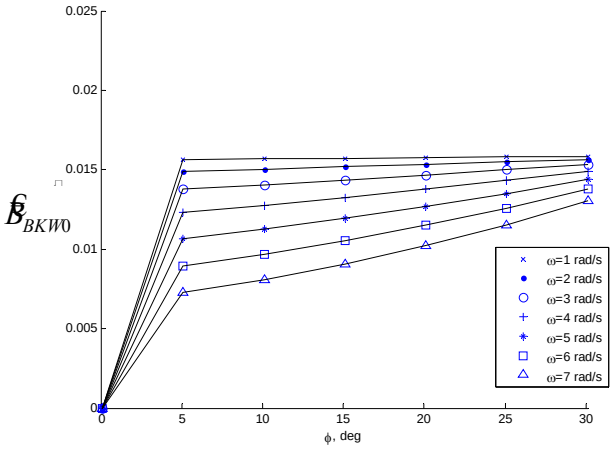

Figure 15. Approximation for the cargo ship bilge keel wave-making component as a function of roll amplitude, $Fn = 0$.

4.4 Bilge Keel Wave-Making Component

A simple model for the bilge keel wave-making component was used to suggest the influence of roll amplitude, roll frequency, and bilge keel size on roll damping. The model was only applied to the cargo ship (Figure 15) and Series 60 (Figure 16) because the empirical model for locating the bilge keels is valid for only for conventional ships where the draft is larger than the bilge radius.

The simple model indicated that the bilge keel wave-making damping is essentially constant as a function of roll amplitude, for the lowest frequency. At the highest frequency, the damping is half that at the lower amplitudes of roll, but it increases with roll amplitude, such that it is approaching that of the lowest frequency for the larger roll amplitudes. With this simple model, it is not possible to tell how significant this component is relative to the bilge keel normal force and bilge keel-hull interaction damping components.

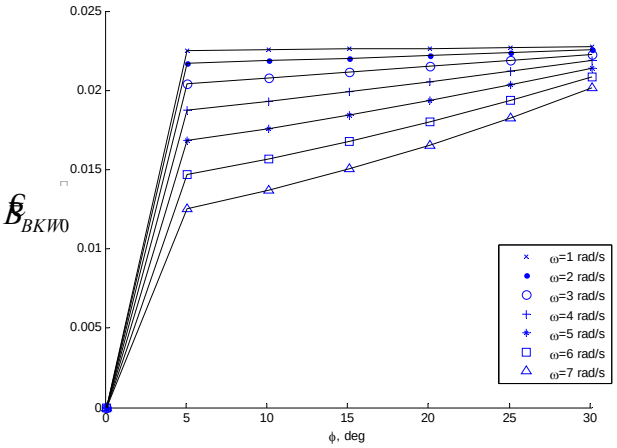

Figure 16. Approximation for the Series 60 bilge keel wave-making component as a function of roll amplitude, $Fn = 0$.

4.5 Effect of Bilge Keel Size and Roll Amplitude on Bilge Keel Damping Components

Because the bilge keel roll damping components are significant portions of the total roll damping, it is important to examine the bilge keel damping model to determine its limitations due to hull proportions, bilge keel size, and roll amplitude.

Larger bilge keels increased the bilge keel normal force damping component and decreased the bilge keel-hull interaction

damping component. This results from the dependency on the Keulegan-Carpenter number used in the formulation of the drag coefficient incorporated in the damping. Both the bilge keel normal force and the bilge keel-hull interaction components increase with increased roll amplitude and roll frequency. However, with larger bilge keels, the bilge keel-hull interaction component reaches a peak value before then decreasing with increasing roll amplitude.

For the hull forms examined, the ratio of the bilge keel-hull interaction component to the bilge keel normal force component exponentially decreases exponentially with increased bilge keel size.

Confirming Ikeda's results (Ikeda, et al., 1978b), at small roll amplitudes, increased bilge keel size resulted in an increase in the bilge keel-hull interaction damping component. For both the Series 60 hull and ONR Topsides Series, with larger bilge keel sizes at larger roll amplitude, the damping peaks and then decreases. In the case of the Series 60 hull, this peak occurs for a bilge keel size well outside of practical designs. In the case of the ONR Topsides Series, the range of the three design bilge keel spans (1.25 m, 1.5 m, and 1.75 m full-scale) shows a decrease in the bilge keel-hull interaction component at larger roll amplitudes. Knowing this behavior with increased bilge keel size is important because many modern ships feature larger bilge keels

The bilge keel normal force component may also have a limitation based on bilge keel size, because of the formulation used for the drag coefficient. From the parameters investigated, it appears that bilge keel size necessary to limit applicability of the formula for this component is outside of the practical range of bilge keel spans used on ships.

A simple formulation was used to examine the bilge keel wave-making damping component at zero speed. This formulation showed an increase in the damping with increased roll amplitude, which was more pronounced for the higher roll frequencies. The damping decreased for increased roll frequency. For the highest frequency, the bilge keel wave-making damping nearly doubled from the 5 degree roll amplitude to the 30 degree roll amplitude (Figures 15 and 16).

Based on the formulation for r and R given by Ikeda, et al. (1978e), the bilge keel is assumed to be attached to the hull at the midpoint of the quarter circle circumscribed by the bilge circle radius (Figure 2). These parameters are used in both the bilge keel normal force and bilge keel-hull interaction components. Although this assumption appears to be adequate for conventional ship types, variation of the deadrise angle on modern ships, such as naval combatants, may invalidate this assumption and necessitate a different formulation. This must also be considered when applying the formulation for the depth of the bilge keel from the free surface to determine the influence of the bilge keel wave-making component.

5. CONCLUSIONS

Bilge keel roll damping predictions were made using Ikeda's component model for three vessels: a cargo ship, Series 60, and the ONR Topside Series hull form. Comparisons were made for all three ships to highlight differences in bilge keel roll damping for modern hull-form geometries and to identify limits for application.

The bilge keel-hull interaction damping component is limited by both bilge keel size and roll amplitude. A simple formulation for the bilge keel wave-making damping was presented to identify when this term should be considered in the calculation of the total bilge keel damping.

Using this formulation, for larger roll amplitudes and larger bilge keel sizes the relative increase in bilge keel wave-making

damping suggest that accurate computations of this component must be made using an exact model so that its significance relative to the bilge keel normal force and bilge keel-hull interaction damping components can be determined. As part of these computations, the bilge keel added mass contribution to the roll moment of inertia of the entire vessels should be examined.

Ikeda's method was the first comprehensive model developed to determine roll damping and components were devised to represent physical phenomena contributing to roll damping. These frequency-domain components are used to determine equivalent linear damping for time-domain implementation (Ikeda, et al., 1978e; Himeno, 1981). The component model has been shown to be sufficient for conventional hull forms at small roll angles.

Although substantial work has been performed to extended the applicability of the component analysis model, the semi-empirical nature of the formulation may result in difficulties particularly for ships with differing hull form proportions, and for physical phenomena in more severe seas, such as the interaction of the bilge keel and free surface and deck submergence, which may significantly alter the roll damping characteristics for a given ship. An improved understanding of these differences and the limitations of the current models will enable further efforts to increase the robustness of applicability of ship roll damping models.

6. ACKNOWLEDMENTS

The authors are grateful for the support of the work presented in this paper from Dr. Pat Purtell, under ONR Program Element 0601153N, and from Dr. John Barkyoumb and the NSWCCD Independent Applied Research (IAR) program, under Program Element 0602123N. We also appreciate the discussions with and useful suggestions from Dr. Leigh McCue of Virginia Tech.

7. REFERENCES

Atsavapranee, P., J. B. Carneal, D. Grant, and A. S. Percival, 2007, "Experimental Investigation of Viscous Roll Damping on the DTMB Model 5617 Hull Form," Proc. 26th International Conference on Offshore Mechanics and Arctic Engineering, San Diego, CA.

Bassler, C., 2007, "Roll Damping Models: Applications to Wave-Piercing Tumblehome Hull Forms," Proc. 28th American Towing Tank Conference, Ann Arbor, MI.

Bassler, C., 2008a, "Application of Parametric Roll Criteria to Naval Vessels," Proc. 10th International Ship Stability Workshop, Daejeon, Korea, 23-25 March.

Bassler, C., 2008b, "Roll Damping Mechanisms for a Wave-Piercing Tumblehome Hull Form," Proc. 6th Osaka Colloquium on Seakeeping and Stability of Ships, Osaka, Japan.

Bassler, C., J. Carneal, and P. Atsavapranee, 2007, "Experimental Investigation of Hydrodynamic Coefficients of a Wave-Piercing Tumblehome Hull Form," Proc. 26th International Conference on Offshore Mechanics and Arctic Engineering, San Diego, CA.

Beck, R. F. and A. M. Reed, 2001, "Modern Computational Methods for Ships in a Seaway," Trans. SNAME, Vol. 109, 1-51.

Bishop, R. C., W. Belknap, C. Turner, B. Simon, and J. H. Kim, 2005, "Parametric Investigation on the Influence of GM, Roll damping, and Above-Water Form on the Roll Response of Model 5613. NSWCCD-50-TR-2005/027.

Blok, J. J. and A. B. Aalbers, 1991, "Roll Damping Due to Lift Effects on High Speed Monohulls," Proc. FAST '91.

Cotton, B. and K. J. Spyrou, 2000, "Experimental and Theoretical Studies of Large Amplitude Ship Rolling and Capsize," Proc. 7th International Conference on Stability of Ships and Ocean Vehicles, February, Launceston, Australia

Dalzell, J. F., 1978, "A Note on the Form of Ship Roll Damping," J. Ship Research, 22(3).

de Kat, J., 1988, "Large Amplitude Ship Motions and Capsizing in Severe Sea Conditions," Ph.D. Thesis, University of California, Berkeley.

EMB, 1920, "Revised Report of Pitching and Roll Experiments on a Model of Battle Cruisers 1 to 6: With and Without Bilge Keels," United States Experimental Model Basin, January.

EMB, 1931, "Rolling in Waves: Effect of Variations of Form on Roll," United States Experimental Model Basin, Report No. 303, June.

Etebari, A., P. Atsavapranee, C. Bassler, and J. Carneal, 2008, "Experimental Analysis of Rudder Contribution to Roll Damping," Proc. 27th International Conference on Offshore Mechanics and Arctic Engineering, Estoril, Portugal.

Gersten, A., 1969, "Roll Damping of Circular Cylinders With and Without Appendages," Naval Ship Research and Development Center, Report 2621.

Gersten, A., 1971, "Scaling Effects in Roll Damping," Proc. 16th American Towing Tank Conference, Sao Paulo, Brazil, August.

Grant, D. J., A. Etebari, and P. Atsavapranee, 2007, "Experimental Investigation of Roll and Heave Excitation and Damping in Beam Wave Fields," Proc. 26th International Conference on Offshore Mechanics and Arctic Engineering, San Diego, CA.

Haddara, M. R., 1973, "On Nonlinear Rolling of Ships in Random Seas," International Shipbuilding Progress, 20.

Hayden, D. D., R. C. Bishop, J. T. Park, and S. M. Laverty, 2006, "Model 5514 Capsize Experiments Representing the Pre-Contract DDG51 Hull Form at End of Service Life Conditions," NSWCCD-50-TR-2006/020, April.

Himeno, Y., 1981, "Prediction of Ship Roll Damping-State of the Art," Dept. of Naval Architecture and Marine Engineering, Univ. of Michigan, Report 239.

Ikeda, Y., Y. Himeno, and N. Tanaka, 1978a, "On Roll Damping Force of Ship- Effect of Friction on Hull and Normal Force of Bilge Keels," Report of the Department of Naval Architecture, University of Osaka Prefecture, No. 00401.

Ikeda, Y., K. Komatsu, Y. Himeno, and N. Tanaka, 1978b, "On Roll Damping Force of Ship- Effect of Hull Surface Pressure Created by Bilge Keels," Report of the Department of Naval Architecture, University of Osaka Prefecture, No. 00402.

Ikeda, Y., Y. Himeno, and N. Tanaka, 1978c, "On Eddy Making Component of Roll Damping Force on Naked Hull," Report of the Department of Naval Architecture, University of Osaka Prefecture, No. 00403.

Ikeda, Y., Y. Himeno, and N. Tanaka, 1978d, "Components of Roll Damping of Ship at Forward Speed," Report of the Department of Naval Architecture, University of Osaka Prefecture, No. 00404.

Ikeda, Y., Y. Himeno, and N. Tanaka, 1978e, "A Prediction Method for Ship Roll Damping," Report of the Department of Naval Architecture, University of Osaka Prefecture, No. 00405.

Ikeda, Y. and T. Katayama, 2000, "Roll Damping Prediction Method for a High-Speed Planing Craft," Proc. 7th International Conerence on the Stability of Ships and Ocean Vehicles, Tasmania, Australia.

Ikeda, Y., 2004, "Prediction Methods of Roll Damping of Ships and Their Application to Determine Optimum Stabilization Devices," Marine Technology, 41(2), April.

IMO, 2008, "Draft Terminology for the New Generation Intact Stability Criteria," International Maritime Organization SLF 51/WP.2, Annex 2, 16 July.

Katayama, T., T. Taniguchi, and M. Kotaki, 2008, "A Study on Viscous Effects of Roll Damping of a High-Speed Catamaran and a High-Speed Trimaran," Proc. 6th Osaka Colloquium on Seakeeping and Stability of Ships, Osaka, Japan.

Kato, H., 1958, "On the Frictional Resistance to the Rolling Ships," J. Society of Naval Architects of Japan, 102 (in Japanese).

Kato, H., 1965, "Effect of Bilge Keels on the Rolling of Ships," Memoirs of the Defence Academy, Japan, 4.

Keulegan, G. M. and L. H. Carpenter, 1958, "Forces on Cylinders and Plates in an Oscillating Fluid," J. Research of the National Bureau of Standards, 60.

Korpus, R. A. and J. M. Falzarano, 1997, "Prediction of Viscous Ship Roll Damping by Unsteady Navier-Stokes Techniques," J. Offshore Mechanics and Arctic Engineering, 119, pp. 108-113.

Lewison, G. R.G., 1976, "Optimum Design of Passive Roll Stabilizer Tanks," The Naval Architect.

Martin, M., 1958, "Roll Damping Due to Bilge Keels," Iowa University Institute of Hydraulic Research, Report.

Miller, R., J. J. Gorski, and D. J. Fry, 2002, "Viscous Roll Predictions of a Circular Cylinder with Bilge Keels," Proc. 24th Symp. on Naval Hydrodynamics, Fukuoka, Japan.

Miller, R. W., C. C. Bassler, P. Atsavapranee, and J. J. Gorski, 2008, "Viscous Roll Predictions for Naval Surface Ships Appended with Bilge Keels Using URANS," Proc. 27th Symp. on Naval Hydrodynamics, Seoul, South Korea.

Roddier, D., S. W. Liao, and R. W. Yeung, 2000, "On Freely-Floating Cylinders Fitted with Bilge Keels," Proc. 10th International Offshore and Polar Engineering Conference.

Sasajima, H., 1954, "On the Action of Bilge Keels in Ship Rolling," J. Society of Naval Architects of Japan, 86 (in Japanese).

Schmitke, R. T., 1978, "Ship Sway, Roll, and Yaw Motions in Oblique Seas," Trans. SNAME, Vol. 86 pp. 26-46.

Seah, R. K. M., 2007, "The SSFSRVM Computational Model for Three-Dimensional Ship Flows With Viscosity," Ph.D. Dissertation, University of California Berkeley.

Seah, R. K. M. and R. W. Yeung, 2008, "Vortical-Flow Modeling for Ship Hulls in Forward and Lateral Motion," Proc. 27th Symp. on Naval Hydrodynamics, Seoul, South Korea.

Spyrou, K. J. and J. M. T. Thompson, 2000, "Damping Coefficients for Extreme Rolling

and Capsize: An Analytical Approach," J. Ship Research, 44(1).

Stefun, G.. P., 1955, "The Roll Damping of a Cylinder with Half-Circular Sections," David Taylor Model Basin, Hydromechanics Laboratory Technical Note, No. 10-55.

Tanaka, N., 1957, 1958, 1959, 1961, "A Study on the Bilge Keel- Part 1-4," J. Society of Naval Architects of Japan, 101, 103, 105, 109 (in Japanese).

Todd, F. H., 1953, "Some Further Experiments on Single-Screw Merchant Ship Forms," Trans. SNAME, Vol. 61 pp. 516-589.

Vugts, J. H., 1968, "The Hydrodynamic Coefficients for Swaying, Heaving, and Rolling of Cylinders in a Free Surface," NSRC Report 112S.

Wilson, R. V., P. M. Carrica, F. Stern, 2006, "Unsteady RANS Method for Ship Motions with Application to Roll for a Surface Combatant," Computers and Fluids, 35, pp. 501-524.

Yeung, R. W, S. W. Liao, and D. Roddier, 1998, "Hydrodynamic Coefficients of Rolling Rectangular Cylinders," International J. Offshore and Polar Engineering, 8(4).

Yeung, R. W., D. Roddier, B. Alessandrini, L. Gentaz and S. W. Liao, 2000, "On the Roll Hydrodynamics of Cylinders Fitted with Bilge Keels," Proc. 23rd Symp. on Naval Hydrodynamics.

8. APPENDIX: BILGE KEEL DAMPING COMPONENT EQUATIONS

8.1 Bilge Keel Normal Force

The formulation for the bilge keel normal force component of roll damping was given in Ikeda, et al. (1978a). The bilge keel normal force component at zero speed, B_{BKN0}, is given by

$$B_{BKN0} = \frac{8}{3\pi}\rho r^2 {b_{BK}}^2 \omega f^2 \left[\frac{22.5}{\pi f} + 2.4\frac{r\phi}{b_{BK}}\right] \quad (12)$$

where ρ is the fluid density, r is the distance from the roll axis to the bilge keel, b_{bk} is the bilge keel span, ω is the roll frequency, ϕ is the roll angle, and f is an empirical function of the section coefficient,

$$r = d\sqrt{\left(H_0 - \left(1-\frac{\sqrt{2}}{2}\right)\frac{R}{d}\right)^2 + \left(1 - \frac{OG}{d} - \left(1-\frac{\sqrt{2}}{2}\right)\frac{R}{d}\right)^2} \quad (13)$$

and the radius of the bilge circle, R, is

$$R = \begin{Bmatrix} B/2 & H_0 < 1 \\ d & H_0 > 1 \end{Bmatrix} \quad (14)$$

and

$$f = 1 + \left(0.3 \cdot \exp\left(-160\{1-\sigma\}\right)\right) \quad (15)$$

The total bilge keel normal force component, B_{BKN}, is given by

$$B_{BKN} = B_{BKN0} + \frac{\pi}{2}\rho {b_{BK}}^2 r^2 U \quad (16)$$

8.2 Bilge Keel-Hull Interaction

The formulation for the bilge keel-hull interaction component of roll damping was given in Ikeda, et al. (1978b). The bilge keel-hull interaction component, B_{BKH}, is given by

$$B_{BKH} = \frac{4}{3\pi} r^2 d^4 f^2 \omega\phi \int C_p \cdot ldG \quad (17)$$

$$\int C_p \cdot ldG = \left(-A_3 {C_p}^- + B_3 {C_p}^+\right) \quad (18)$$

$$C_D = C_p^{+} - C_p^{-} \tag{19}$$

where C_p^{+} and C_p^{-} are pressure coefficients on the top and bottom of the bilge keel where it is attached to the hull surface. C_p^{+} was determined empirically by Ikeda, et al. (1978b) based on model tests with conventional ships,

$$C_p^{+} = 1.2 \tag{20}$$

and the drag coefficient, C_D, was based on a zero speed formulation and empirical predictions using the *KC* number.

$$C_D = 22.5\frac{b_{BK}}{rf\phi\pi} + 2.4 \tag{21}$$

therefore,

$$C_p^{-} = -22.5\frac{b_{BK}}{rf\phi\pi} - 1.2 \tag{22}$$

The additional coefficients in the pressure coefficient term are given as

$$A_3 = (m_3 + m_4)m_8 - m_7^2 \tag{23}$$

$$B_3 = \frac{m_4^3}{3(H_0 - 0.215\cdot m_1)} + \frac{(1-m_1)^2(2m_3 - m_2)}{6(1-0.215\cdot m_1)} + m_1(m_3 m_5 + m_4 m_6) \tag{24}$$

where

$$m_1 = \frac{R}{d} \quad m_2 = \frac{OG}{d} \quad m_3 = 1 - m_1 - m_2$$
$$m_4 = H_0 - m_1, \tag{25}$$
$$m_5 = \frac{0.414H_0 + 0.0651\cdot m_1^2 - (0.382H_0 + 0.0106)\cdot m_1}{(H_0 - 0.215\cdot m_1)(1-0.215\cdot m_1)}$$
$$m_6 = \frac{0.414H_0 + 0.0651\cdot m_1^2 - (0.382 + 0.0106H_0)\cdot m_1}{(H_0 - 0.215\cdot m_1)(1-0.215\cdot m_1)}$$
$$m_7 = \begin{cases} \dfrac{S_0}{d} - 0.25\pi\cdot m_1 & S_0 > 0.25\pi R \\ 0 & S_0 \le 0.25\pi R \end{cases}$$
$$m_8 = \begin{cases} m_7 + 0.414\cdot m_1 & S_0 > 0.25\pi R \\ m_7 + \sqrt{2}\left(1 - \cos\left(\dfrac{S_0}{R}\right)\right)m_1 & S_0 \le 0.25\pi R \end{cases}$$

$$S_0 = (0.3\pi fr\phi) + 1.95b_{BK} \tag{26}$$

8.3 Bilge Keel Wave-Making: Derivation of the Bilge Keel Depth

The distance from the free surface to the bilge keel, d_{BK}, is given by

$$d_{BK}(\phi) = r\sin(\beta - \phi) \tag{27}$$

where β is the angle between r and the free surface for the condition of the ship without heel (Figure 2). Based on the formulation for r and R given by Ikeda, et al. (1978e), the bilge keel is assumed to be attached to the hull at the midpoint of the quarter circle circumscribed by the bilge circle radius. The assumption appears to be adequate for conventional hull forms, where the draft is larger than the bilge radius, but is not applicable for more modern ship types, where the draft is equal or smaller than the bilge radius. The angle β can be determined by

$$\beta = \tan^{-1}\left(\frac{2d}{B}\right) \tag{28}$$

Using the angle-difference trigonometric relation and the fundamental trigonometric identities, substituting β into (27) gives the following for d_{BK}

$$d_{BK}(\phi) = r\cdot\left[\left(\frac{(2d/B)}{\sqrt{1+(2d/B)^2}}\right)\cos\phi - \sin\phi\cdot\left(\frac{1}{\sqrt{1+(2d/B)^2}}\right)\right] \tag{29}$$

where d is the draft; B the beam; and ϕ the roll angle.